

*Supporting Information for*

**Theoretical framework and experimental methodology to elucidate the  
supersaturation dynamics of nanocrystal growth**

Paul Z. Chen<sup>†</sup>, Aaron J. Clasky<sup>†</sup>, and Frank X. Gu<sup>†,‡,\*</sup>

<sup>†</sup>Department of Chemical Engineering & Applied Chemistry, University of Toronto, Toronto,  
Ontario M5S 3E5, Canada

<sup>‡</sup>Institute of Biomedical Engineering, University of Toronto, Toronto, Ontario M5S 3G9, Canada

Corresponding author: [f.gu@utoronto.ca](mailto:f.gu@utoronto.ca)

This supporting information file includes:

Experimental section

Supplementary text

S1. Kinetics of NC growth via absorbance and color

S2. Theoretical modeling of NC growth

S3. Development of the simulated supersaturation profile

Supplementary Figures S1–S8

Supplementary Tables S1–S4

## **Experimental section**

### **Materials and methods**

Gold(III) chloride hydrate ( $\text{HAuCl}_4 \cdot x\text{H}_2\text{O}$ ,  $x \approx 3$ ; >99.995%), sodium bromide ( $\text{NaBr}$ , >99.99%), cetyltrimethylammonium bromide (CTAB, >99%), cetyltrimethylammonium chloride (CTAC, >99%), L-ascorbic acid (>99.0%), sodium borohydride ( $\text{NaBH}_4$ , >99.99%), sodium hydroxide ( $\text{NaOH}$ , >98%), hydrochloric acid ( $\text{HCl}$ , 37%), thiol-terminated polystyrene (PS-thiol, 5 kDa, polydispersion index  $\leq 1.1$ ), tetrahydrofuran (THF, 99.9%) and toluene (99.8%) were purchased from Sigma-Aldrich (Oakville, ON, Canada). Unless otherwise specified, MilliQ water (18.2  $\text{M}\Omega \cdot \text{cm}$  at 25 °C; Milli-Q® Reference Water Purification System; MilliporeSigma, Oakville, ON, Canada) was used for the experiments. Quartz cuvettes (volume: 20 ml, path length: 1 cm) were purchased from Thermo Fisher Scientific (Ottawa, ON, Canada). Scintillation vials (20 ml) were purchased from VWR International (Mississauga, ON, Canada). Reagents were used as received.

### **Nanoseed preparation**

The synthesis procedures were adapted from Park et al.<sup>1</sup> In a 20 ml scintillation vial, 10 mM  $\text{HAuCl}_4$  (250  $\mu\text{l}$ ) was added to a solution of CTAB (100 mM, 9.75 ml), followed by the rapid addition of ice-cold  $\text{NaBH}_4$  (10 mM, 600  $\mu\text{l}$ ). Samples were stirred at room temperature for 2 min at 1400 rpm and then placed in an incubator at 27°C for 3 h to nucleate nanoseeds. Samples were brown in color, indicating small colloidal NCs. To further grow the nanoseeds, CTAC (200 mM, 2 ml), ascorbic acid (100 mM, 1.5 ml), the above nanoseed solution (50  $\mu\text{l}$ ), and  $\text{HAuCl}_4$  (0.5 mM, 2 ml) were added sequentially to a 20 ml scintillation vial and stirred at room temperature for 15 min at 300 rpm. The color progressed to red and had an extinction peak around 520 nm, indicating growth to a diameter of 10 nm.<sup>1,2</sup> Samples were then twice centrifuged (20,600 x g for 30 min)

and resuspended. The first resuspension was with MilliQ water (1 ml), and the second was with CTAC (20 mM, 1 ml).

### **Nanocube synthesis**

In a 20 ml quartz cuvette, CTAC (100 mM, 6 ml), NaBr (40 mM, 30  $\mu$ l), nanoseeds (30  $\mu$ l), HCl or NaOH (200  $\mu$ l of the solutions described below), L-ascorbic acid (10 mM, 390  $\mu$ l, dropwise) and HAuCl<sub>4</sub> (0.5 mM, 6 ml) were added sequentially and then mixed via pipette. After this initial pipette mixing step, the solution was left untouched for the rest of synthesis. The concentration of HCl or NaOH added was modified according to the sample: 0.1 equiv. of NaOH (1.5 mM, 200  $\mu$ l), 1 equiv. of HCl (15 mM, 200  $\mu$ l), or 2 equiv. of HCl (30 mM, 200  $\mu$ l), in which molar equivalent (equiv.) refers to the molar ratio between the added reagent and added Au.

### **Arresting colloidal NC growth**

At various times during synthesis, the growth of colloidal NCs was arrested via ligand exchange and solvent transfer based on a procedure adapted from Park et al.<sup>3</sup> Nanocubes were prepared as previously described with 0.1 equiv. of NaOH. At various time points, 8 ml of colloidal NCs was quickly added to a THF solution of PS-thiol (1.1 mM, 10 ml) in a 20 ml scintillation vial. This solution was vortexed aggressively (>2 min) until it became grey and translucent. This procedure was used for each time point (30 s, 45 s, 2 min, 4 min, 7 min, and 15 min). Samples were left at room temperature overnight to allow the colloidal NCs to settle in the vial. After this, most of the liquid was removed from the vial via pipetting, and vials were placed under reduced pressure until the liquid had evaporated (>2 h). Next, toluene (1 ml) was added to each sample, followed by sonication to resuspend the NCs. Samples were then twice centrifuged (21,000xg for 25 min) and resuspended. The first and second resuspensions were with 1.0 and 0.1 ml of toluene, respectively.

### **Optical characterization of NC growth**

Nanocubes were synthesized in quartz cuvettes (volume: 20 ml, path length: 1 cm) as described above. To characterize growth via extinction, the cuvettes were placed in darkness in an apparatus, which passed light from a source (OceanOptics, Orlando, USA) using fiber optic cables (OceanView Optics, Orlando, USA), 10-m round subminiature assembly (SMA) connectors and detector collection lenses (L4 chamfered; OceanView Optics, Orlando, USA) to an in-line UV/Vis spectrometer (Flame T spectrometer; OceanView Optics, Orlando, USA) with a 4000-series detector (350-1000 nm filter; OceanView Optics, Orlando, USA). Extinction spectra (400-900 nm, step size: 0.217 nm) were collected every 30 s. The initial scan was taken immediately after H<sub>Au</sub>Cl<sub>4</sub> was added which initiated growth, and this image was considered the start time (0 s) in kinetic analyses. To characterize growth via nanoplasmonic color, the cuvettes were imaged (EOS Rebel T7i with an EF 100 mm macro lens, Canon Canada, Inc., Toronto, ON, Canada) under fume hood lighting every 30 s or 1 min. The initial image was taken immediately after H<sub>Au</sub>Cl<sub>4</sub> was added which initiated growth, and this image was considered the start time (0 s) in kinetic analyses.

### **Scanning transmission electron microscopy**

STEM samples were prepared by drop casting the respective solution (5  $\mu$ l) on a 400-mesh pure C, Cu grid (Ted Pella, Inc., Redding, USA) and dried under hood evaporation. Before drop casting, colloidal NCs were prepared via centrifugation and resuspension in MilliQ. Grids were cleaned with ultraviolet light (5-15 min per side) using a ZoneTEM (Hitachi High-Technologies Canada Inc, Etobicoke, ON, Canada) sample cleaner before imaging. HAADF-STEM and SE-STEM images were acquired in vacuo using a Hitachi HF-3300 300 kV Environmental TEM with an electron acceleration voltage of 300 kV.

## NC counting and sizing

For counting, three representative large-area HAADF-STEM images were assessed to determine the shape of each NC in these micrographs, yielding  $n \geq 550$  NCs characterized for its shape distribution for each sample. For sizing, two representative large-area HAADF-STEM images were analyzed using ImageJ (version 1.51s; National Institutes of Health, USA), yielding  $n \geq 40$  NCs sized for each time point. Each cube or icosahedra that could be clearly identified in the HAADF-STEM images were sized. For cubes, four measurements were taken for each NC: two corner-to-corner ( $C$ ) and two edge-to-edge ( $E$ ) measurements (Fig. S3a†). For cuboctahedra, three side-to-side ( $D$ ) measurements were taken (Fig. S3b†). Sizing data were presented as mean values of these measurements for each NC in Fig. S4†. For a perfectly sharp nanocube,  $C = E\sqrt{2}$  based on the parameters described in Fig. S3†, where  $C = \text{smax}(C1, C2)$  and  $E = \text{min}(E1, E2)$ . To delineate truncated cubes from cubes,<sup>1</sup> we applied a factor threshold of 1.3; that is, truncated cubes ( $C < 1.3E$ ) were below this threshold, whereas cubes ( $C \geq 1.3E$ ) were equal to or above it. The count for each shape was summed from these images, and yields were presented as percentages of the overall number of NCs counted. The sharpness index ( $S$ ) of the nanocubes was measured in units of nm and  $d_{111}$ , in which  $d_{111}$  denotes  $\{111\}$  interplanar distances (the corners of face-centered cubic nanocubes point in the  $\langle 111 \rangle$  direction<sup>4</sup>).

## Kinetics characterization and modeling

The peak absorbance values between 500-600 nm were used to analyze the absorbance kinetics. The parameters used to characterize the kinetics of colloidal NC growth and to theoretically model growth are summarized in Table S2†. Coefficients of determination ( $r^2$ ) were calculated when fitting to  $C_{\text{NC}}(t)$  from eq (14) for these reactions. Further information on the methods for kinetics

characterization and modeling is described in the Supporting Information. Modeling was performed using Matlab R2021a (MathWorks, Inc, Natick, MA, USA).

## Supplementary text

### **S1. Kinetics of NC growth via absorbance and color**

Throughout the entire reaction to grow colloidal Au nanocubes, we took absorbance spectra or color images through the synthesis cuvette (see the Experimental Section for additional information on methods). We then analyzed the absorbance or colorimetric kinetics. More specifically, the absorbance kinetics were analyzed using

$$\% \text{ Yield } [\text{Au}^0]_{\text{NC},i} = \frac{A_i - \min(\mathbf{A})}{\max(\mathbf{A}) - \min(\mathbf{A})} \quad (\text{S1})$$

where  $A_i$  represents the peak absorbance at time  $i$  and  $\max(\mathbf{A})$  and  $\min(\mathbf{A})$  represent the maximum and minimum peak absorbance, respectively, throughout the reaction. The absorbance spectra were collected using the in-line spectrometer (Experimental Section) and the peak absorbance refers to the highest absorbance value at the peak wavelength between 500-600 nm. The full spectra along the time course of the reaction are shown in Figure 3c.

Since the nanoplasmonic color of the colloidal NCs in this reaction was red (Figure S1a), we used the G value from red-green-blue (RGB) analysis of these color images (ImageJ, version 1.51s; National Institutes of Health, USA). The intrinsic variation among images in white balance across images was normalized using  $G_{N,i} = G_{\text{NC},i} - G_{B,i}$ , where, for the  $i$ th image,  $G_{N,i}$  represents the normalized G value,  $G_{\text{NC},i}$  represents the G value from the colloidal NC formulation, and  $G_{B,i}$  represents the G value from the white background. The colorimetric kinetics were then analyzed using

$$\% \text{ Yield } [\text{Au}^0]_{\text{NC},i} = \frac{\max(\mathbf{G}_N) - G_{N,i}}{\max(\mathbf{G}_N) - \min(\mathbf{G}_N)} \quad (\text{S2})$$

where  $\max(\mathbf{G}_N)$  and  $\min(\mathbf{G}_N)$  represent the maximum and minimum normalized G values for the array of images, respectively, over the reaction.

This seed-mediated synthesis had an induction period at the beginning of, and sigmoidal shape to, the reaction. As such, the absorbance and colorimetric kinetics were fitted to eq (14), and 100% Yield  $[\text{Au}^0]_{\text{NC},i}$  was taken to be  $C_T - C_0$  when the results were presented in units of concentration rather than % yields. In both cases, equation fitting determined the variable parameters,  $k_g$  and  $t_0$ . Along with the constants summarized in Table S2†, these fitted parameters were inputted into eq (15) to develop a continuous, temporal function that was then inputted into eq (8), estimating the supersaturation dynamics in the reaction.

## S2. Theoretical modeling of NC growth

We used the temporal profile of supersaturation to model the growth of the colloidal Au nanocubes. We inputted the constants listed in Table S2† along with the supersaturation profile derived from the absorbance kinetics into eq (4) to determine the theoretical growth rate at each time point  $i$ . We approximated cuboctahedra, truncated cubes, and cubes in our model as pseudospherical NCs, with the radius as the side-to-side length for cube shapes. Since the molar concentration of  $\text{Br}^-$  was low in the growth formulation,  $C_0$  was estimated based on the equilibrium concentration of  $[\text{AuCl}_2]^-$ , based on a previous approach to determine  $C_0$  for the monomer of a NC growth reaction.<sup>5</sup> In this seed-mediated growth reaction,  $n_{\text{NC}}$  was estimated based on the measured peak optical density of the seed ( $OD_{\text{peak}} = 0.78$  for nanocubes that were diluted 3x in MilliQ water) and the expected particle concentration for the seed, 10-nm nanocuboctahedra<sup>1, 2</sup> (<https://www.sigmaaldrich.com/CA/en/technical-documents/technical-article/materials-science-and-engineering/biosensors-and-imaging/gold-nanoparticles>), and we took  $n_{\text{NC}}$  as approximately

$2.1 \times 10^{11}$ . Since the supersaturation profile and growth rate were discretized in the modeling code, we chose a small time step ( $\Delta t$ ) between each time point in the array to approximate a continuous function for the arrays for the supersaturation profile, growth rate, and NC size. The seed size (i.e., the initial size at  $t_1 = 0$ ) was taken to be 10 nm,<sup>1,2</sup> and we multiplied the growth rate at each time  $i$  by  $\Delta t$  to determine the NC size at time  $i + 1$ . This procedure was continued for the duration of the reaction, building a high-resolution contiguous growth profile for these NCs. The code generated during this study, including the script used to characterize supersaturation and model growth, is available at GitHub (<https://github.com/paulzchen/supersaturation>).

Our analyses considered that our seed-mediated synthesis reaction grew NCs without additional homogenous nucleation. Such nucleation produces small nuclei as the pre-existing NCs grow in seed-mediated syntheses, meaning that nucleation can be identified by a broadening distribution of NC sizes throughout the reaction. We analyzed the sizes of cuboctahedral and cubic NCs at various times throughout the reaction (Fig. S4†), which showed that there were no additional small nuclei that emerged during our reaction. Moreover, we used a weak-reducing agent (L-ascorbic acid) and CTAC at concentrations that have been shown to inhibit homogenous nucleation within the time frame of our reaction.<sup>1,2</sup>

### **S3. Development of the simulated supersaturation profile**

To further investigate how supersaturation dynamics influenced the growth profile of the NCs, we developed an artificially simulated profile of the supersaturation. More specifically, we sought to understand if the complex supersaturation dynamics determined by our framework were appropriate. Thus, we aimed to develop a supersaturation profile that more resembled that expected when considering the LaMer-Dinegar model.<sup>6</sup> Our characterization of the supersaturation

dynamics most differed from the LaMer-Dinegar model in the initial phase of rapid monomer consumption (phase **i** in Figure 3e), which arose largely from the dependence on  $1/r(t)$  for the factor multiplying  $R_{\text{NC}}(t)$  in eq (8). Hence, we set  $r$  as a constant value in this factor to remove the initial phase in the artificially simulated supersaturation profile. The choice of this constant  $r$  was made to result in theoretical sizes, as determined by eq (4) and the procedure described above, that matched those of the experimental NCs by the end of growth. This led to the desired artificial supersaturation profile that indeed resembled how supersaturation would be expected to progress according to simpler dynamics, such as expected when considering the LaMer-Dinegar model. The code generated during this study, including the script used to artificially simulate supersaturation and model growth based on this profile, is available at GitHub (<https://github.com/paulzchen/supersaturation>).

## Supplementary Figures

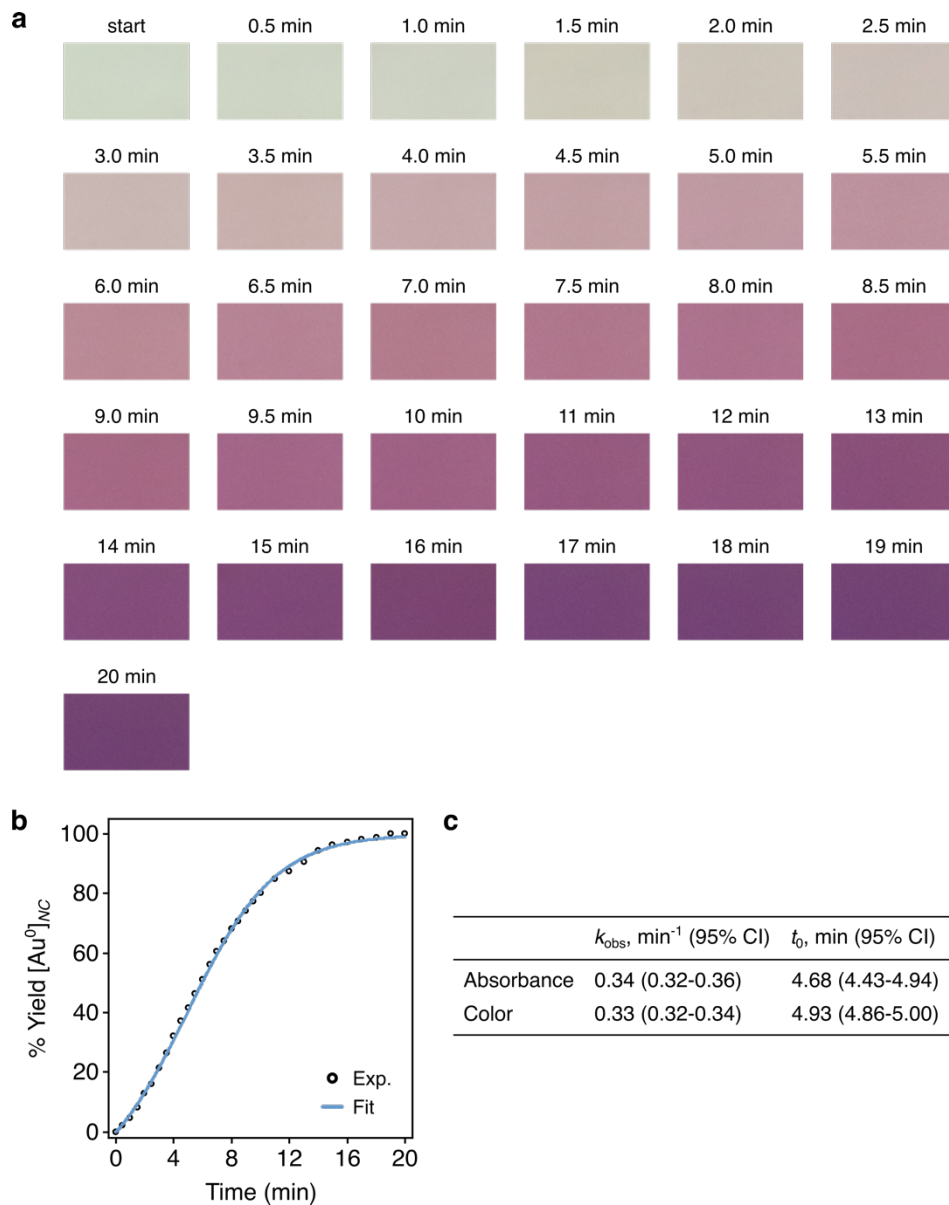


**Figure S1.** Kinetics of NC growth analyzed via nanoplasmonic color development. (a) Time-resolved images of nanoplasmonic color throughout the growth of colloidal Au nanocubes. (b) Kinetics of NC growth analyzed via the colors in (a). The data were fitted to Eq. (11) ( $r^2 > 0.99$ ). (c) Comparison of colloidal NC growth kinetics based on absorbance and colorimetric images. CI, confidence interval.

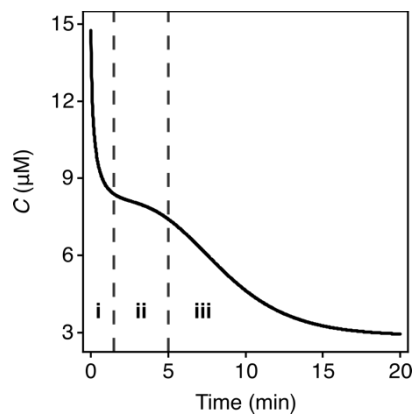


**Figure S2.** Estimated concentrations of monomer throughout growth. This profile was estimated using eq. (1) and the profile of the supersaturation dynamics shown in Figure 3e.

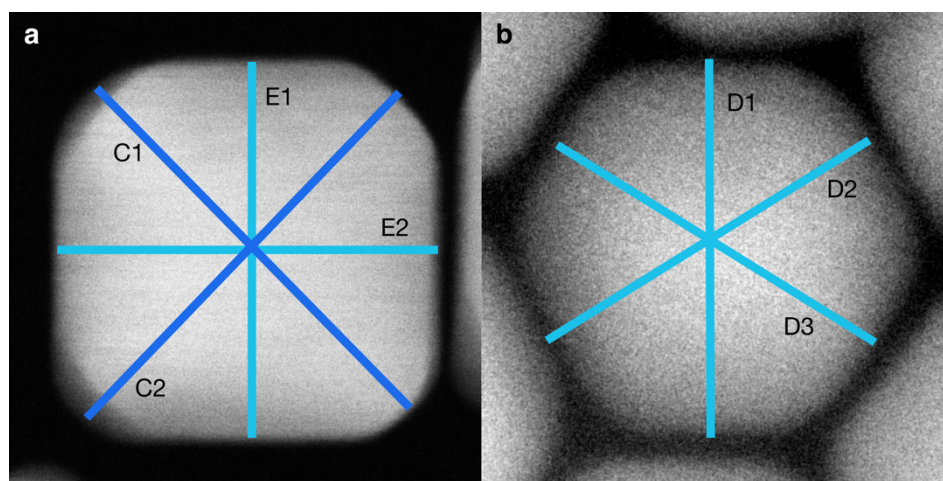


**Figure S3.** Schematic representations of NC sizing measurements from STEM images. (a) Cubes were characterized by two corner-to-corner (*C*) and two edge-to-edge (*E*) distances. (b) Cuboctahedra were characterized by three side-to-side (*D*) distances.

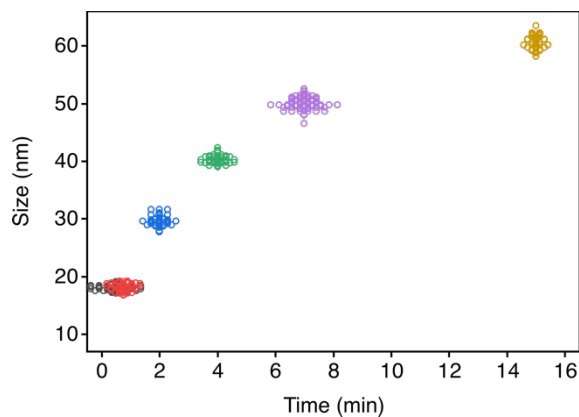


**Figure S4.** Raw sizing data for cuboctahedral and cubic NCs. Each data point represents the sizing of one NC, and sized was conducted at 30 s, 45 s, 2 min, 4 min, 7 min, and 15 min (from left to right). The data were spread horizontally to show overlapping points. The mean and SD of the experimental data at each time point are shown in Fig. 3f and Fig. S5b†.

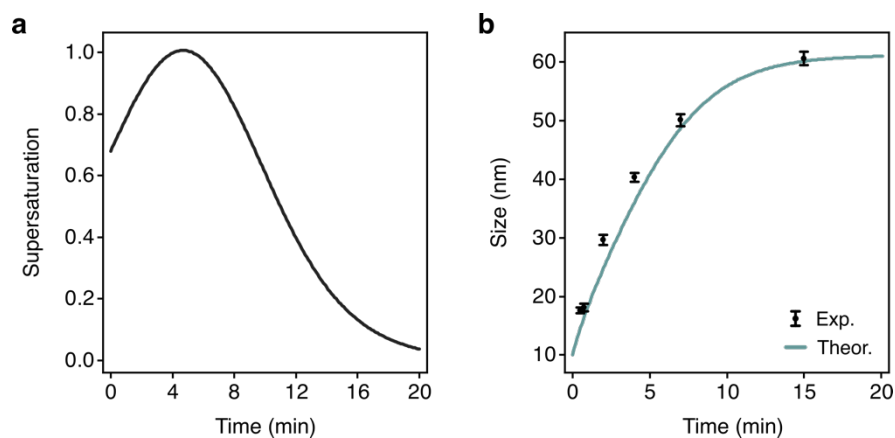


**Figure S5.** Simulated supersaturation dynamics without an initial stage of high supersaturation and the resulting predicted growth profile. (a) Profile of simulated supersaturation dynamics. (b) Theoretical growth profile based on the simulated supersaturation profile from (a) and eq (4). The model was overlaid on experimental sizes for the colloidal nanocubes throughout growth. This supersaturation profile was simulated such that the final nanocube size concurred with that which was experimentally observed.

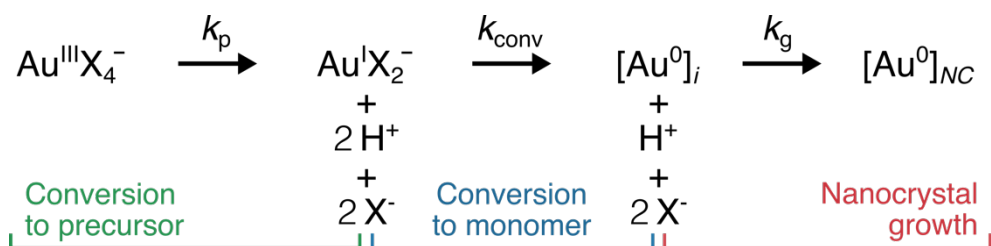


**Figure S6.** Reduction pathway of Au during colloidal NC synthesis. X = halide, which is predominantly  $\text{Cl}^-$  and small quantities of  $\text{Br}^-$  in our growth formulation. Both reaction mechanisms for Au reduction, disproportionation and direct reduction, result in the same stoichiometry for the produced monomer,  $\text{H}^+$  and  $\text{X}^-$ . The rate constants  $k_p$ ,  $k_{\text{conv}}$ , and  $k_g$  are for the conversion to precursor, conversion to monomer, and NC growth, respectively. The addition of  $\text{H}^+$  and  $\text{Cl}^-$  left-shifts the reaction, decreasing the concentration of monomer.

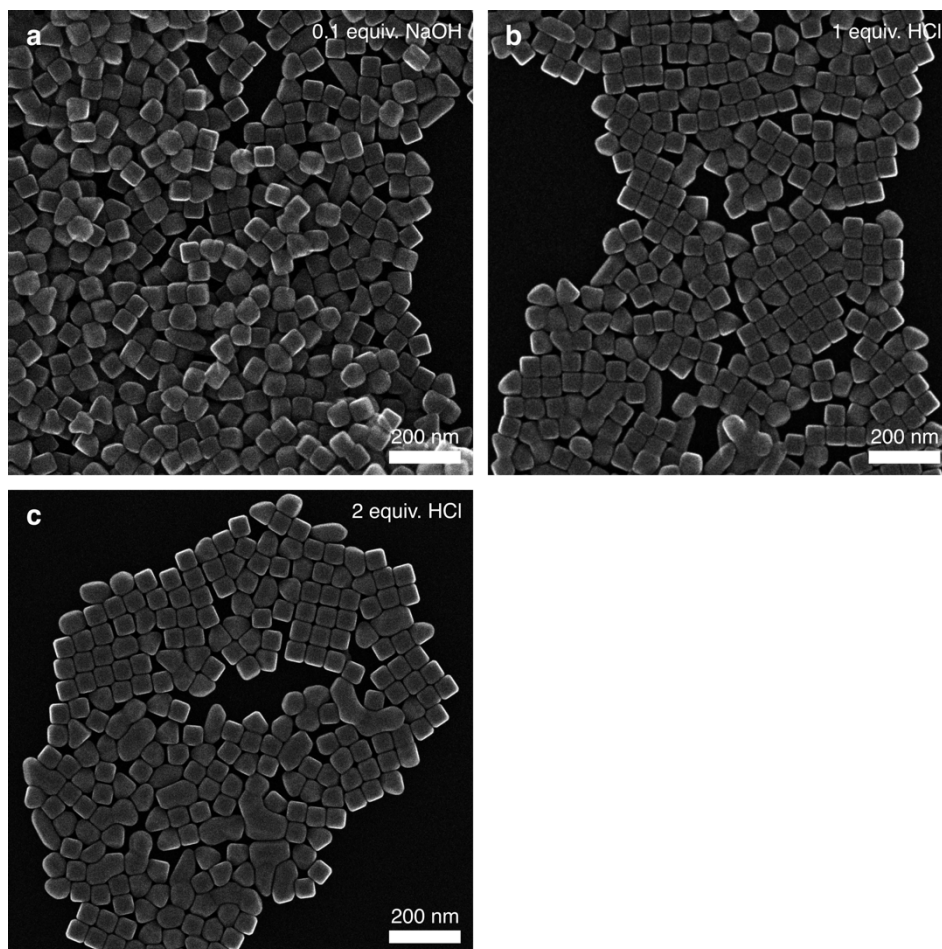


**Figure S7.** Large-area SE-STEM images of Au nanocubes after growth. The micrographs show the NCs grown with (a) 0.1 equivalents (equiv.) of NaOH, (b) 1 equiv. of HCl, or (c) 2 equiv. of HCl.

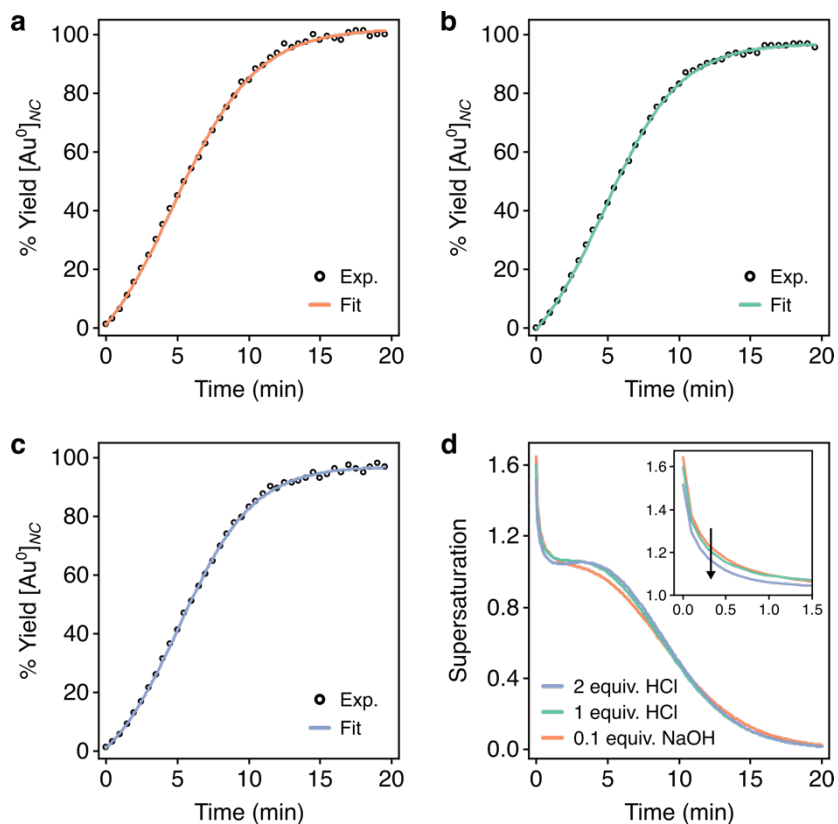


**Figure S8.** Kinetics of NC growth analyzed via the peak nanoplasmonic absorbance. Colloidal Au nanocubes were grown with (a) 0.1 equivalents (equiv.) of NaOH, (b) 1 equiv. of HCl or (c) 2 equiv. of HCl. The data were fitted to eq (14) ( $r^2 > 0.99$  for each). (d) Temporal profile of supersaturation dynamics throughout the reactions shown in (a) to (c). Inset, supersaturation dynamics during the first phase of rapid monomer consumption. The arrow denotes lower early supersaturation with more HCl added.

## Supplementary Tables

**Table S1.** Summary of the parameters used to develop the theoretical framework.

Symbol*	Definition	Units
$\sigma$	Supersaturation	-
$C$	Monomer concentration	mol L <sup>-1</sup>
$C_0$	Saturation concentration of the monomer	mol L <sup>-1</sup>
$\Delta\mu$	Chemical-potential difference between a monomeric unit and an integrated crystal unit	eV
$k_B$	Boltzmann constant	J K <sup>-1</sup>
$N_A$	Avogadro's number	mol <sup>-1</sup>
$T$	Temperature of the synthesis formulation	K
$k_{\text{conv}}$	Rate constant for the conversion of precursor to monomer	s <sup>-1</sup>
$k_g$	Rate constant for growth	s <sup>-1</sup>
$k_p$	Rate constant for the conversion to precursor	s <sup>-1</sup>
$k_{\text{dis}}$	Rate constant for monomer dissolution	s <sup>-1</sup>
$r$	Nanocrystal radius	m
$v_c$	Molar volume of Au	m <sup>3</sup> mol <sup>-1</sup>
$\gamma$	Surface energy	J m <sup>-2</sup>
$R$	Gas constant	J mol <sup>-1</sup> K <sup>-1</sup>
$C_i$	Monomer concentration at the nanocrystal interface	mol L <sup>-1</sup>
$D$	Bulk diffusion coefficient of the monomer or precursor	m <sup>2</sup> s <sup>-1</sup>
$k_0^g$	Rate constant for growth of a flat ( $r \rightarrow \infty$ ) interface	m s <sup>-1</sup>
$\delta$	Thickness of the stagnant layer	m
$R_{\text{NC}}$	Intensive rate of monomer integration into nanocrystals	mol L <sup>-1</sup> s <sup>-1</sup>
$t$	Time	s
$\alpha$	Transfer coefficient of growth	-
$J$	Monomer flux onto the surface of a nanocrystal	mol s <sup>-1</sup>
$n_{\text{NC}}$	Total number of nanocrystals undergoing growth	-
$V_s$	Volume of the synthesis formulation	L
$A$	Optical attenuation	-
$c$	Concentration of nanocrystals or monomer in the nanocrystals	mol L <sup>-1</sup>
$l$	Sample path length	m
$\varepsilon$	Extinction coefficient of the nanocrystals	L mol <sup>-1</sup> m <sup>-1</sup>
$C_T$	Total concentration of usable monomer added to the reaction	mol L <sup>-1</sup>
$C_{\text{NC}}$	Concentration of monomers integrated in nanocrystals	mol L <sup>-1</sup>
$t_0$	Inflection time in the Boltzmann sigmoid function	s

\*Parameters are listed around their order of inclusion in the main body.

† $c$  represents either the concentration of particles ( $n_{\text{NC}}/V_s$ ) or the concentration of monomer in the NCs ( $C_{\text{NC}}$ ) depending on the synthesis reaction.

**Table S2.** Parameters used to characterize supersaturation and model colloidal NC growth.

Symbol	Definition	Units	Value
$v_c$	Molar volume of Au	$\text{cm}^3 \text{mol}^{-1}$	10.3
$C_0$	Saturation concentration of $[\text{Au}^0]_i$	$\mu\text{M}$	2.87 (ref. <sup>5</sup> )
$C_T$	Total concentration of monomer added	$\mu\text{L}^{-1}$	
$D$	Bulk diffusion coefficient of monomer/precursor	$\text{m}^2 \text{s}^{-1}$	$9.0 \times 10^{-10}$ (ref. <sup>7</sup> )
$n_{\text{NC}}$	Number of seeds added to growth formulation	-	$2.1 \times 10^{11}$
$V_s$	Volume of the synthesis formulation	mL	12.5
$d_i$	Size of the seeds added to the growth formulation	nm	10.0
$k_B$	Boltzmann constant	$\text{J K}^{-1}$	$1.381 \times 10^{-23}$
$T$	Temperature of synthesis formulation	K	293.15
$N_A$	Avogadro's number	$\text{mol}^{-1}$	$6.022 \times 10^{23}$
$l$	Sample path length	cm	1

**Table S3.** Summary of shape evolution throughout colloidal nanocube growth.

Time (min)	Shape distribution (%)					
	Cuboctahedra	Truncated cubes	Cubes	Overgrown cubes	Other shapes	Total cubes/cuboctahedra
0.5	96.3	0.0	0.0	0.0	3.7	96.3
2.0	0.0	77.4	5.3	10.2	7.1	92.9
4.0	0.0	74.0	3.3	15.0	7.7	92.3
7.0	0.0	34.7	35.5	21.9	7.9	92.1
15	0.0	8.6	60.0	24.4	7.0	93.0

**Table S4.** Summary of kinetics and size for colloidal nanocubes when grown with various formulations.

Sample	$k_{\text{obs}}, \text{min}^{-1}$ (95% CI)	$t_0, \text{min}$ (95% CI)	Size, nm (SD)
0.1 equiv. NaOH	0.34 (0.32-0.36)	4.68 (4.43-4.94)	63.9 (0.89)
1 equiv. HCl	0.37 (0.36-0.39)	4.72 (4.58-4.87)	62.8 (1.04)
2 equiv. HCl	0.38 (0.37-0.40)	5.10 (4.95-5.25)	61.2 (1.39)

## References

1. J. E. Park, Y. Lee and J. M. Nam, *Nano Lett.*, 2018, **18**, 6475-6482.
2. Y. Zheng, X. Zhong, Z. Li and Y. Xia, *Part. Part. Syst. Character.*, 2014, **31**, 266-273.
3. K. Park, L. F. Drummy, R. C. Wadams, H. Koerner, D. Nepal, L. Fabris and R. A. Vaia, *Chem. Mater.*, 2013, **25**, 555-563.
4. H. G. Liao, D. Zherebetsky, H. Xin, C. Czarnik, P. Ercius, H. Elmlund, M. Pan, L. W. Wang and H. Zheng, *Science*, 2014, **345**, 916-919.
5. S. A. Morin, M. J. Bierman, J. Tong and S. Jin, *Science*, 2010, **328**, 476-480.
6. V. K. Lamer and R. H. Dinegar, *J. Amer. Chem. Soc.*, 1950, **72**, 4847-4854.
7. M. Harada, K. Okamoto and M. Terazima, *J. Colloid Interf. Sci.*, 2009, **332**, 373-381.